The electrical and thermal conductivity and thermopower of nickel doped compounds $(Ni_xTi_{1-x})_{1+y}S_2$ at low temperatures

2006 J. Phys. D: Appl. Phys. 39 1230

(http://iopscience.iop.org/0022-3727/39/6/033)

INSTITUTE OF PHYSICS PUBLISHING JOURNAL OF PHYSICS D: APPLIED PHYSICS
J. Phys. D: Appl. Phys. **39** (2006) 1230–1236 doi:10.1088/0022-3727/39/6/033

The electrical and thermal conductivity and thermopower of nickel doped compounds $(Ni_xTi_{1-x})_{1+y}S_2$ at low temperatures

J Zhang, X Y Qin[1], D Li and H Z Dong

Key Laboratory of Materials Physics, Institute of Solid State Physics, Chinese Academy of Sciences, 230031 Hefei, People's Republic of China

E-mail: xyqin@issp.ac.cn

Received 22 November 2005, in final form 10 January 2006
Published 3 March 2006
Online at stacks.iop.org/JPhysD/39/1230

Abstract

Nickel doped compounds $(Ni_xTi_{1-x})_{1+y}S_2$ ($0 \leqslant x \leqslant 0.06$) were prepared by solid-state reaction, and their dc electrical and thermal conductivity and thermopower were investigated from 5 K to 310 K. The results indicated that Ni doping caused a metal-like to semiconductor-like behaviour transition; at low temperatures ($T <\sim 100$ K) dc electrical conduction σ for $(Ni_xTi_{1-x})_{1+y}S_2$ ($x > 0$) obeys Mott's 2D variable range hopping law, $\ln \sigma \propto T^{-1/3}$, indicating that TiS_2 possesses 2D transport characteristics. The appearance of Mott's 2D law could originate from potential disorder introduced by Ni substitution for Ti in S–Ti–S slabs, while the metal-to-semiconductor transition can be ascribed to de-degeneration through reduction in electron concentration due to Ni substitution. Experiments also indicated that both lattice thermal conductivity and carrier (mainly electron) thermal conductivity of the doped compounds decreased upon doping, which can be explained as the combined effects of substitution with intercalation of Ni and reduction of carrier concentration upon doping, respectively. The absolute Seebeck coefficient $|S|$ was found to decrease after doping, which could be attributed to generation of some holes after Ni substitution for Ti. The figure of merit, ZT, of the doped compounds $(Ni_xTi_{1-x})_{1+y}S_2$ ($x > 0$) decreased as compared with TiS_2 due to both a large increase in their resistivity and an obvious decrease in their Seebeck coefficient.

1. Introduction

TiS_2 has an anisotropic structure with a trigonal space group, $P\bar{3}m$. It is known to exist in two polytypes ($1T$, $2H$) with octahedral and trigonal prismatic coordinations, respectively. The main difference between the $1T$-TiS_2 and $2H$-TiS_2 layers is the type of the local coordination of the metal: octahedral ($1T$) versus trigonal-prismatic ($2H$) [1]. The most stable form of TiS_2 ($1T$-TiS_2 crystallizes in a layered CdI_2-like structure) consists of sheets of face-sharing TiS_6 octahedra forming S–Ti–S sandwich layers, where a Ti sheet is sandwiched between two sulfur sheets. Atoms within S–Ti–S sheets are bound by strong covalent interactions; bonding between the layers is determined by weak van der Waals forces.

Although the structure of TiS_2 is quite simple, the nature of the electronic structure of the layered material, TiS_2, has been in dispute over the past decades. Up to now, for instance, whether it is a semiconductor or semi-metal has not been clarified [2–16]. Through measurements of the Hall coefficient, Seebeck coefficient and resistivity as a function of pressure, Klipstein and Friend [2] found that the band overlap between S 3p states and Ti 3d states increased at

[1] Author to whom any correspondence should be addressed.

the rate of 4.5 meV kbar^{-1} and concluded that TiS_2 is a semiconductor with a gap of 0.18 ± 0.06 eV. The optical measurements of Greenway and Nitsche [3] indicated that TiS_2 is a semiconductor with a gap of 1–2 eV. Chen *et al* [4] and Barry *et al* [5] reported a band gap of about 0.3 eV from angle-resolved photoemission studies (ARPS). Photoemission experiments by Shepherd and Williams [6] indicate a band gap of less than 0.5 eV. Calculations using the pseudopotential (PP) method [7] also indicated that TiS_2 is a semiconductor with an indirect band gap of about 2 eV. On the contrary, some theoretical calculations indicate that TiS_2 is a semi-metal. Lately Benesh *et al* [8] got a semi-metallic ground state for TiS_2 by using the LAPW method as a function of pressure. Similarly, band calculations based on the augmented spherical wave (ASW) method by Fang *et al* [9], the linear-muffin-tin-orbital (LMTO) method by Wu *et al* [10–12] and the FP-LAPW method [13, 14] showed that TiS_2 possessed a semi-metallic ground state. Meanwhile, many experiments [15,16] indicated that the electrical resistivity of TiS_2 almost exclusively exhibits metallic behaviour, decreasing with decreasing temperature down to nearly 0 kelvin. So far, no semiconductor behaviour in the electrical conductivity of TiS_2 has ever been observed experimentally. Hence, it is interesting and also significant (as mentioned below) for one to clarify the observed contradictory phenomena concerning the properties of TiS_2.

On the other hand, layered-structured TiS_2 is well known for its capability of intercalation by a wide range of both organic and inorganic materials into its van der Waals gap [17]. Since Li^+ can easily intercalate and leave the van der Waals gap of TiS_2, it has been studied as a promising cathode material for rechargeable lithium-ion batteries [18–20]. Besides Li [2, 21, 22], transition metals, such as Fe, Co and Ni [23], have been successfully inserted into the gap of TiS_2, and the influences of this intercalation on the physical properties of the corresponding compounds were investigated and explored. In particular, Imai *et al* reported that TiS_2 had a large Seebeck coefficient, S, and power factor (S^2/ρ, ρ is electrical resistivity) at room temperature [24], indicating that TiS_2 is a potential candidate for thermoelectric applications. Very recently, the work in our group indicated that a large enhancement of thermoelectric properties for TiS_2 could be realized by proper Bi interaction into its van der Waals gap [25].

As outlined above, in order to tailor the physical properties of TiS_2, numerous studies conducted so far concentrated mainly on intercalation of guest atoms or molecules. Alternatively, at least in principle, the properties of TiS_2 can also be tuned by doping in the S–Ti–S sheets of TiS_2 with foreign atoms. The aim of the present work is to synthesize the nickel doped compounds $(Ni_xTi_{1-x})_{1+y}S_2$, and to investigate the effect of Ni doping on their electrical and thermal transport properties and thermopower in the temperature range from 5 K to 310 K.

2. Experiments

Polycrystals of nickel doped compounds $(Ni_xTi_{1-x})_{1+y}S_2$ samples with nominal $x = 0$, 0.02, 0.04, 0.06 were prepared by the solid-state reaction method. Elementary nickel (99.99 wt%), titanium (99.99 wt%) and sulfur (99.999 wt%) powders were weighed accurately to give the desired composition, mixed intimately to give a homogeneous mixture and sealed in an evacuated quartz tube, which was heated (in a horizontal furnace) at a heating rate of 0.5 K min^{-1} to 880 K and kept for 7 days to obtain powder samples. The phase structures and the compositions of the obtained samples were checked using x-ray powder diffraction (XRD) and energy dispersive spectroscopy (EDS), respectively. XRD analysis was carried out on a Philips diffractometer using Cu-Kα radiation. The accurate lattice parameters were determined from the d-values of the XRD peaks using a standard least-squares refinement method with a Si standard for calibration.

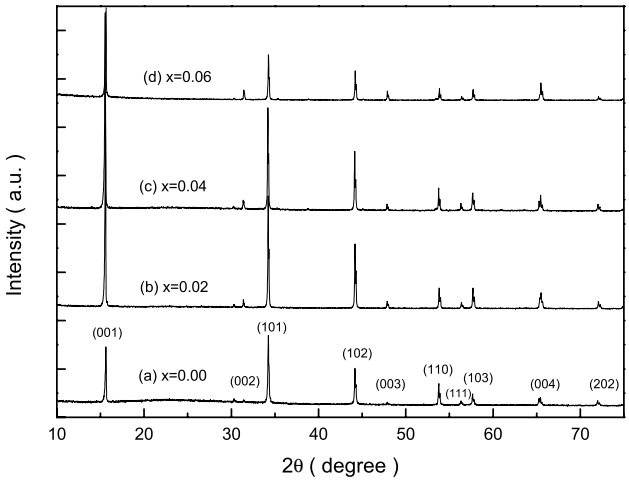

Figure 1. The XRD patterns for the synthesized specimens with different Ni contents x. ((a) $x = 0$, (b) $x = 0.02$, (c) $x = 0.04$ and (d) $x = 0.06$).

To measure their thermoelectric properties, the synthesized powders were compacted by hot-pressing (under a pressure of 300 MPa) in vacuum at 673 K to obtain bulk samples of size $30 \times 10 \times (\sim)1.5\,mm^3$. Then bar-shaped specimens of size $13 \times 3 \times (\sim)1.5\,mm^3$ were cut from the bulk samples for the measurements. Four probes (Cu straps) were electrically and thermally attached to the specimens by silver conductive adhesive paste (Phentex Corp. USA) to measure their dc resistance, and when thermopower and thermal conductivity were measured the two probes in the middle were used to explore temperature gradient (difference) and potential difference. All the thermoelectric properties (dc resistance, thermopower and thermal conductivity) were measured simultaneously using a physical property measurement system (PPMS, Quantum Design, USA) in the temperature range from 5 K to 310 K. Carrier concentration was determined by measurements of the Hall coefficient at room-temperature in a field, $H = 0.73$ T.

3. Results and discussions

3.1. Phase determination and change of lattice parameters after Ni addition

Figure 1 shows XRD patterns for the synthesized specimens with different Ni content x. One can see from figure 1 that all the main peaks on the XRD patterns match well those for TiS_2, indicating that the doped specimens have the same crystallographic structure as that of TiS_2. The values of the lattice parameters a and c for all the samples have been

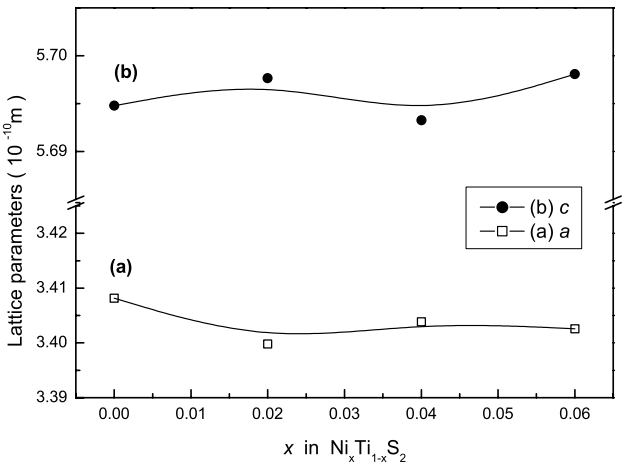

Figure 2. Variation of the lattice parameters a and c versus Ni content, x.

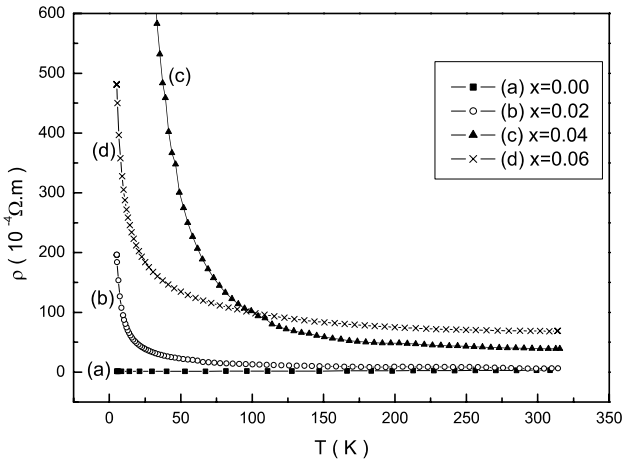

Figure 3. Dependence of the electrical resistivity ρ on temperature for TiS_2 and for Ni doped compounds $(Ni_xTi_{1-x})_{1+y}S_2$ ((a) $x = 0$, (b) $x = 0.02$, (c) $x = 0.04$ and (d) $x = 0.06$).

calculated from the XRD data, which are shown in figure 2. It can be seen that the lattice parameter c increases from 5.6948 Å to 5.6981 Å with increasing nickel content x from 0 to 0.06. In contrast, the lattice parameter a is found to decrease from 3.4081 Å to 3.4026 Å as nickel content x increases from 0 to 0.06. Many investigations [26–28] showed that the lattice parameter a of the intercalated compounds M_xTiS_2 (here M stands for intercalated elements) was always found to increase with increasing content of intercalated elements (for example, lattice parameter a changed from 3.4083 Å to 3.4156 Å in Bi_xTiS_2 [26] with x increasing from 0 to 0.25; the parameter a of Li_xTiS_2 [27] changed from 3.407 Å to 3.452 Å with increasing x from 0 to 1.0; parameter a of self-intercalated compound $Ti_{1+x}S_2$ [28] increased from 3.405 Å to 3.412 Å with x increasing from 0 to 0.1). Therefore, the decrease in parameter a shows that the substitution of Ni (for Ti) has occurred after the Ni addition, as the atomic radius of nickel is smaller than that of Ti, and if Ni atoms replace Ti atoms to form covalent bonds [29] the lattice would shrink as compared with that of pristine TiS_2. However, the increase in parameter c after Ni doping suggests that accompanying the substitution of Ni for Ti some Ni or/and Ti atoms have intercalated into the van der Waals gap of TiS_2. Hence, the samples synthesized in the present experiments can be expressed as $(Ni_xTi_{1-x})_{1+y}S_2$.

3.2. The effect of doping with Ni on dc resistivity

The dc electrical resistivity versus temperature for $(Ni_xTi_{1-x})_{1+y}S_2$ ($x = 0, 0.02, 0.04, 0.06$) in the range 5–310 K is presented in figure 3. One can see that the ρ–T curve for the pure TiS_2 sample ($x = 0$) shows a metal-like behaviour (i.e. $d\rho/dT > 0$) in the whole temperature range investigated. Fitting the resistivity to a power law, $(\rho(T) - \rho_0) \propto T^{\gamma}$, gives $\gamma = 2.2$, in agreement with previous results reported by Klipstein *et al* [30]. In contrast, the ρ–T curves for the doped compounds ($x = 0.02$, $x = 0.04$, $x = 0.06$) show a semiconductor-like behaviour (i.e. $d\rho/dT < 0$) in the whole temperature range investigated. This is quite in contrast to that for purely intercalated compounds, M_xTiS_2, whose metallic behaviour is enhanced after the intercalation of guest elements [25, 31, 32], indicating further that substitution of Ni for Ti has taken place in the compounds. In other words, the present result indicates that a transition from metal-like to semiconductor-like behaviour occurs after doping with Ni in TiS_2. In addition, the electrical resistivity of Ni doped compounds $(Ni_xTi_{1-x})_{1+y}S_2$ ($x > 0$) is greater than that of pure TiS_2 and increases monotonously with increasing Ni content at the temperature, $T >\sim 100$ K, which is in contrast to the phenomena observed in purely intercalated TiS_2, where its resistivity always decreased with increasing content of intercalated elements, as observed in Bi_xTiS_2 [25] and Li_xTiS_2 [31, 32].

The reason why $(Ni_xTi_{1-x})_{1+y}S_2$ transits from metallic behaviour ($x = 0$) to semiconducting behaviour ($x > 0$) after doping with Ni may lie in the fact that TiS_2 is a semiconductor with a narrow band gap [33]. However, in practice, self-intercalation of Ti into TiS_2 is unavoidable in the synthesis process [28]. As a result, TiS_2 appears almost always as an extrinsic semiconductor. Moreover, if ionization energy of the self-intercalation Ti atoms is small enough, complete ionization will occur at the low temperatures that can be reached normally. If the number of intercalated Ti atoms (acting as donors) is sufficiently large, a degenerate semiconductor will form which behaves metallically, just as observed normally in TiS_2. As the substitution of Ni for Ti occurred in the doped compounds, acceptors (Ni^{2+}) will be introduced. Then the carrier (electron) concentration will decrease if a compensation effect takes place. Consequently, as Ni content (number of acceptors) is high enough, de-degeneration of TiS_2 will occur, leading to the appearance of the semiconductor behaviour. In fact, the Hall coefficient measurements indicated that (see figure 4) the carrier concentration n (assuming the major carriers are electrons) decreased catastrophically from 2.3×10^{20} cm^{-3} for $x = 0$ to $\sim 1 \times 10^{18}$ cm^{-3} for $x = 0.04$ (then n increased slightly as Ni content increased further mainly due to increased contribution from intercalation). The present result strongly suggests that Ni substitution for Ti would reveal the nature of TiS_2 as a narrow semiconductor, which was covered by its metallic behaviour resulting from a high degree of degeneration.

Considering that some Ni substitution for Ti in S–Ti–S conduction planes may give rise to potential disorder, which

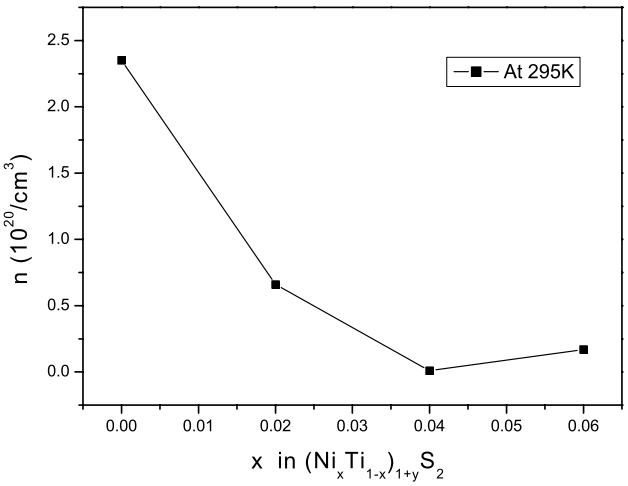

Figure 4. Variation of carrier concentration (at room temperature) with Ni content, x.

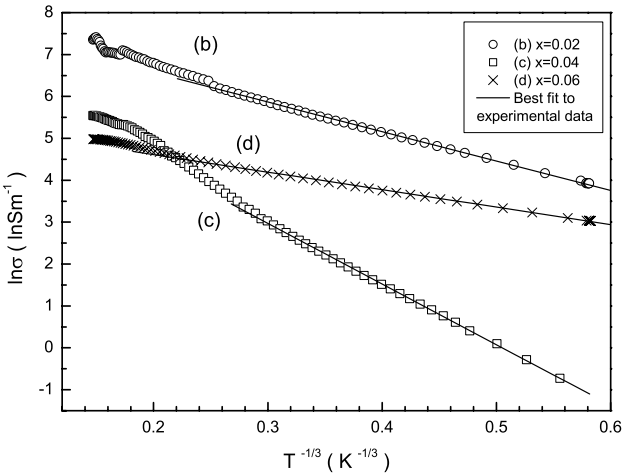

Figure 5. Variation of $\ln\sigma$ versus $1/T^{1/3}$ for Ni doped compounds $(Ni_xTi_{1-x})_{1+y}S_2$ ((b) $x = 0.02$, (c) $x = 0.04$ and (d) $x = 0.06$). The solid lines are the best (linear) fits of the experimental data to formula (1).

would be strong enough to lead to considerable localized states, at very low temperatures phonon assisted tunnelling or hopping may dominate the conduction process. By best fitting the experimental data to Mott's variable range hopping (VRH) law, we find that the conductivity data of $(Ni_xTi_{1-x})_{1+y}S_2$ ($x \geqslant 0.02$) in corresponding low-temperature ranges are in good agreement with Mott's two-dimensional (2D) VRH model, i.e.

$$\sigma = \sigma_0 \exp\left[-\left(\frac{T_0}{T}\right)^{1/3}\right], \qquad (1)$$

where $T_0 = 8/(\pi k N(E_F) l_v^2)$ is the hopping barrier and σ_0 is a constant. Figure 5 shows the plots of $\ln\sigma$ versus $T^{-1/3}$ for the doped specimens. It can be seen that there are good linear relations between $\ln\sigma$ and $T^{-1/3}$ at low temperatures, $T <\sim 100$ K, suggesting that TiS_2 has 2D transport characteristics. The fitted values of T_0 are 476 K, 3892 K and 94 K for $x = 0.02$, 0.04 and 0.06, respectively. Generally, the variation of state density at the Fermi surface is expected not to be very strong upon light doping. Therefore, the increase in T_0

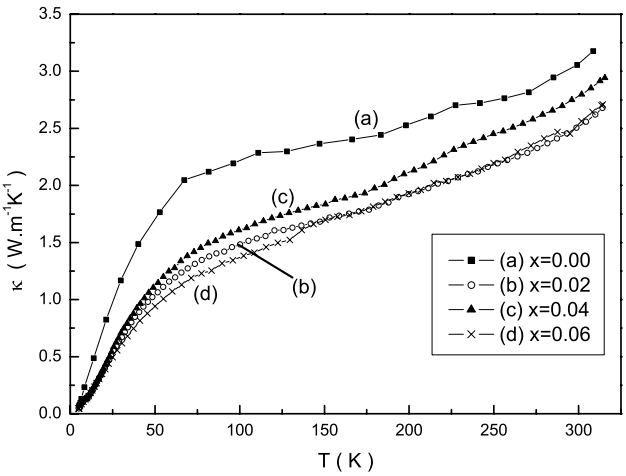

Figure 6. Plot of thermal conductivity κ versus temperature for TiS_2 and for Ni doped compounds $(Ni_xTi_{1-x})_{1+y}S_2$ ((a) $x = 0$, (b) $x = 0.02$, (c) $x = 0.04$ and (d) $x = 0.06$).

with increasing Ni content x ($\leqslant 0.04$) would largely reflect a decrease in localization length, l_v. It is understandable that as Ni content increases the potential disorder would become more significant due to more substitution of Ni atoms for Ti atoms in the periodic crystal. Nevertheless, a very large decrease in T_0 at $x = 0.06$ would reflect an increase in localized state $N(E_F)$ due to heavy doping.

3.3. The effect of doping with Ni on thermal conductivity

The temperature dependences of total thermal conductivity κ for $(Ni_xTi_{1-x})_{1+y}S_2$ are shown in figure 6. It can be seen that doping with Ni causes a decrease in their thermal conductivity. Similarly to that of TiS_2, the thermal conductivity κ of the doped compounds shows weak dependence above 60 K, below which κ of all the compounds increases rapidly and approximately linearly with increasing temperature. The total thermal conductivity κ can be expressed by the sum of the lattice component (κ_L) and electronic component (κ_e) as $\kappa = \kappa_L + \kappa_e$. The κ_e values can be estimated from Wiedemann–Franz's law as $\kappa_e = LT/\rho$ (here L is the Lorentz number and $L = 2.44 \times 10^{-8}\,V^2\,K^{-2}$ for free electrons). Consequently, κ_L can be obtained from κ and κ_e, as shown in figure 7. By comparing figure 6 with figure 7 it can be seen that the values and temperature dependences of lattice conductivity κ_L are similar to those of the total thermal conductivity κ. This result indicates that the thermal conductivity of $(Ni_xTi_{1-x})_{1+y}S_2$ comes mainly from their lattice conductivity. One notices from figure 7 that the lattice thermal conductivity of doped compounds $(Ni_xTi_{1-x})_{1+y}S_2$ ($x > 0$) is obviously smaller than that of pure TiS_2, and usually the higher the doped Ni content, the smaller its lattice conductivity (there is an exception at $x = 0.02$). This decrease of lattice thermal conductivity may originate from: (1) substitution of Ni atoms for Ti atoms, which would cause its lattice thermal conductivity to decrease due to both reduction of mean free path of phonons resulting from distortion of the lattice after this substitution and decrease in acoustic velocity caused by the heavier weight of Ni atoms (than that of Ti atoms); (2) intercalation of some Ni (or/and Ti) atoms, which could cause phonon scattering by low-frequency

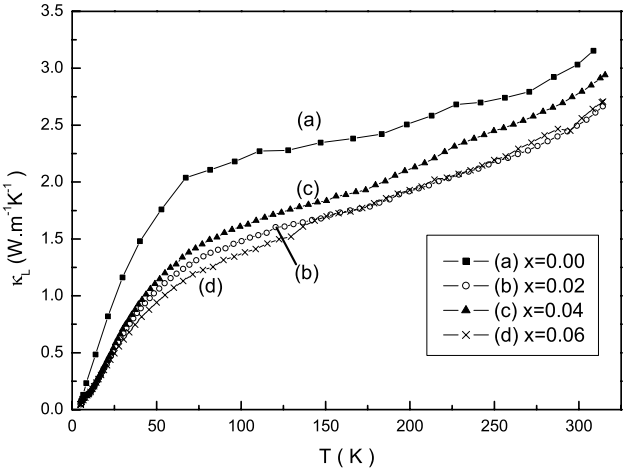

Figure 7. Plot of lattice thermal conductivity κ_L versus temperature for TiS_2, and for Ni doped compounds $(Ni_xTi_{1-x})_{1+y}S_2$ ((a) $x = 0$, (b) $x = 0.02$, (c) $x = 0.04$ and (d) $x = 0.06$).

vibrations, or 'rattling' [25], of the intercalated Ni or/and Ti atoms in the van der Waals gap of TiS_2, as has been shown in Bi_xTiS_2 [25]. By comparison, 'rattling' of the intercalated Ni in the van der Waals gaps of TiS_2 would be more effective in reducing its lattice thermal conductivity than the effects of Ni substitution, which could explain why the thermal conductivity of the compound with $x = 0.02$ is smaller than that of the compound with $x = 0.04$ (figure 7), for there would be a larger portion of Ni atoms intercalating into the van der Waals gaps of TiS_2 in the compound with $x = 0.02$ than in that with $x = 0.04$, which is suggestive from the large increase in the constant c at $x = 0.02$ (see figure 2(b)).

Figure 8(a) shows the thermal conductivity ratio κ_e/κ as a function of temperature for $(Ni_xTi_{1-x})_{1+y}S_2$. It can be seen from this figure that the carrier contribution to total thermal conductivity is substantial in TiS_2; however, in the whole temperature range their contribution decreased in the doped compounds (figure 8(a)). As an illustration, figure 8(b) gives the plot of κ_e/κ at 300 K versus Ni content. We can see that as x increased from 0 to 0.02, κ_e/κ decreased from 0.75% to about 0.48%; then it dropped rapidly to about (or less than) 0.05% as Ni content $x \geqslant 0.04$, having a change tendency similar to that of the carrier concentration (figure 4), which could be mainly ascribed to the decrease in the carrier concentration in $(Ni_xTi_{1-x})_{1+y}S_2$ ($x \neq 0$) as the content of doped Ni increased.

3.4. The effect of doping with Ni on thermopower

The variations of the Seebeck coefficient (S) for $(Ni_xTi_{1-x})_{1+y}S_2$ with temperature are shown in figure 9. The negative values of the Seebeck coefficient observed for all the specimens over the entire temperature range show that the major charge carriers in $(Ni_xTi_{1-x})_{1+y}S_2$ are electrons, as mentioned above. The temperature behaviour of the Seebeck coefficient for the doped compounds $(Ni_xTi_{1-x})_{1+y}S_2$ ($x > 0$) with different Ni contents is more or less similar to that of pristine TiS_2. The absolute Seebeck coefficient $|S|$ for every compound is found to increase with increasing temperature in the whole temperature range investigated. The small valley observed at the temperature around 60 K for each in the plot of

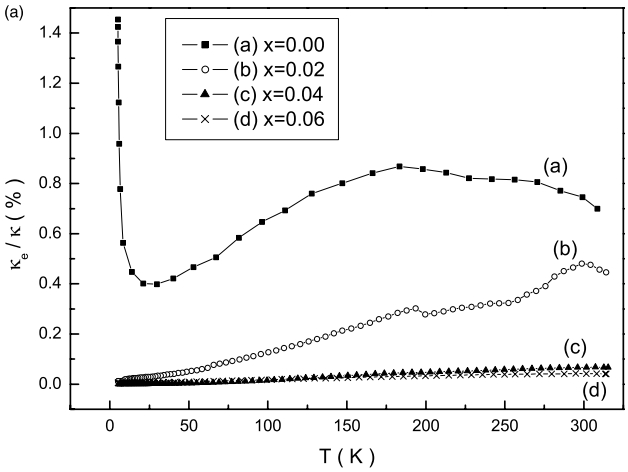

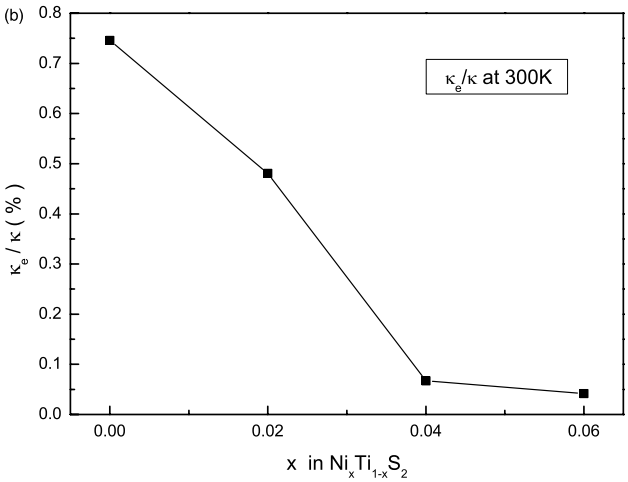

Figure 8. (a) The thermal conductivity ratio κ_e/κ as a function of temperature for $(Ni_xTi_{1-x})_{1+y}S_2$ ((a) $x = 0$, (b) $x = 0.02$, (c) $x = 0.04$ and (d) $x = 0.06$). (b) The plot of κ_e/κ at 300 K versus Ni content x.

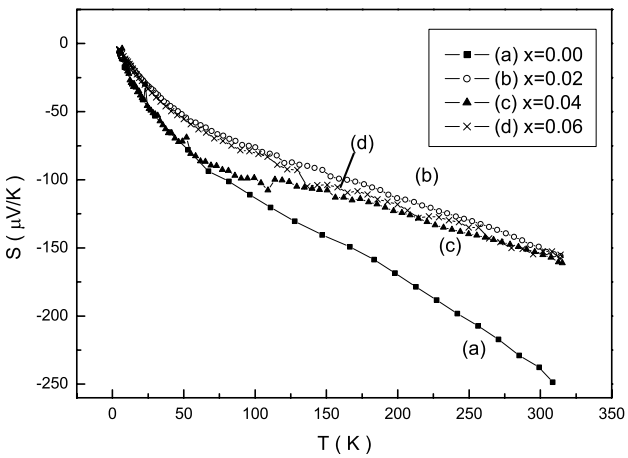

Figure 9. Variation of thermopower S with temperature for TiS_2, and for Ni doped compounds $(Ni_xTi_{1-x})_{1+y}S_2$ ((a) $x = 0$, (b) $x = 0.02$, (c) $x = 0.04$ and (d) $x = 0.06$).

S versus T could be ascribed to the phonon–drag effect [26]. However, one notices from figure 9 that $|S|$ of the doped compounds increases more slowly with temperature than that of pristine TiS_2. At temperatures above 80 K the thermopower

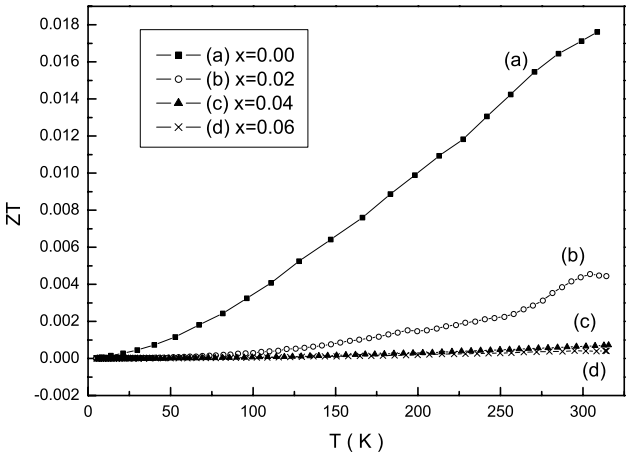

Figure 10. Variation of ZT with temperature for TiS_2, and for Ni doped compounds $(Ni_xTi_{1-x})_{1+y}S_2$ ((a) $x = 0$, (b) $x = 0.02$, (c) $x = 0.04$ and (d) $x = 0.06$).

for $(Ni_xTi_{1-x})_{1+y}S_2$ has an approximately linear relationship to temperature. The diffusive part of thermopower (T-linear thermopower) in the case of the single carriers (electrons) can be described by the formula [26]:

$$S \propto \frac{\pi^2 k^2 T}{e E_F}, \tag{2}$$

where k, e and E_F are the Boltzmann constant, electron charge and Fermi level, respectively. This formula indicates that the slope of the linear portion in the plot S versus T is inversely proportional to the Fermi level. This seems to indicate that the smaller slope of the linear portion in the plot S versus T for $(Ni_xTi_{1-x})_{1+y}S_2$ ($x > 0$) than that for TiS_2 implies greater E_F, which is in contrast to experimental results concerning the large decrease in carrier concentration and the appearance of semiconductor behaviour. This discrepancy, instead, may result from the possibility that Ni substitution for Ti can generate some holes (in the valence band) which produce a positive Seebeck coefficient, leading to a drop in the total $|S|$ due to counteraction of the contributions coming from electrons and holes. Nevertheless, the quantity of the holes from Ni acceptors is expected not to be very large since the decrease of $|S|$ for $(Ni_xTi_{1-x})_{1+y}S_2$ ($x > 0$) as compared with that of TiS_2 is not severe. The present results suggest that the major part of Ni acceptors act as compensation centres, leading to the remarkable decrease in electron concentration and the appearance of semiconductor behaviour.

3.5. The effect of doping with Ni on ZT

The temperature dependences of dimensionless figure of merit ZT (here $Z = S^2/\rho\kappa$) for TiS_2 and the Ni doped compounds $(Ni_xTi_{1-x})_{1+y}S_2$ are shown in figure 10. The ZT values for all the specimens tend to increase with increasing temperature. However, the ZT of doped compounds ($x > 0$) is smaller than that of pure TiS_2 although their thermal conductivity decreases substantially. This decrease in ZT of the doped compounds originates from both large increases in their resistivity and the obvious decrease in their Seebeck coefficient. Therefore, in order to raise the figure of merit ZT of TiS_2 it is necessary for one to adopt light substitution so as not to cause a substantial rise of the resistivity, and it is significant for one to lower thermal conductivity and simultaneously to inhibit the generation of holes in TiS_2.

4. Summary and conclusions

The effects of doping with Ni on transport and thermoelectric properties of $(Ni_xTi_{1-x})_{1+y}S_2$ have been investigated in the temperature range from 5 K to 310 K. The results indicated that Ni doping caused not only the large increase in its dc resistivity but also a transition from metal-like to semiconductor-like behaviour. Moreover, it was found that at low temperatures ($T <\sim 100$ K) the electrical conduction for $(Ni_xTi_{1-x})_{1+y}S_2$ ($x > 0$) obeys Mott's 2D VRH model, indicating that TiS_2 possesses 2D transport characteristics. The metal-to-semiconductor transition can be ascribed to de-degeneration through reduction in electron concentration due to Ni substitution for Ti, while the appearance of Mott's 2D VRH could originate from potential disorder introduced by Ni substitution. Experiments also indicated that both lattice thermal conductivity and carrier (mainly electron) thermal conductivity of the doped compounds decreased upon doping, which can be explained as the combined effects of substitution with intercalation of Ni and reduction of carrier concentration upon doping, respectively. The absolute Seebeck coefficient $|S|$ was found to decrease after doping, which suggests that some holes are generated after Ni substitution for Ti. The figure of merit, ZT, of the doped compounds $(Ni_xTi_{1-x})_{1+y}S_2$ ($x > 0$) decreased as compared with TiS_2 in the whole temperature range investigated, which results from both the large increase in their resistivity and the obvious decrease in their Seebeck coefficient.

Acknowledgments

Financial support from National Natural Science Foundation of China (No 50472097 and No 10504034) is gratefully acknowledged.

References

[1] Ivanovskaya V V and Seifert G 2004 *Solid State Commun.* **130** 175
[2] Klipstein P C and Friend R H 1984 *J. Phys.* C **17** 2713
[3] Greenway D L and Nitsche R T 1965 *Phys. Chem. Solids* **26** 1445
[4] Chen C H, Fabian W, Brown F C, Woo K C, Davies B, DeLong B and Tompson A H 1980 *Phys. Rev.* B **21** 615
[5] Barry J J *et al* 1983 *J. Phys.* C **16** 393
[6] Shepherd F R and Williams P M 1974 *J. Phys.* C **7** 4416
[7] Allan D R, Kelsey A A, Clark S J, Angel R J and Ackland R J 1998 *Phys. Rev.* B **57** 5106
[8] Benesh G A, Woolley A M and Umrigar C 1985 *J. Phys. C: Solid State Phys.* **18** 1595
[9] Fang C M, de Groot R A and Haas C 1997 *Phys. Rev.* B **56** 4455
[10] Wu Z Y, Ouvrard G, Lemaux S, Moreau P, Gressier P and Lemoigno F 1996 *Phys. Rev. Lett.* **77** 2101
[11] Wu Z Y, Lemoigno F, Gressier P, Ouvrard G, Moreau P, Rouxel J and Natoli C R 1996 *Phys. Rev.* B **54** R11009
[12] Wu Z Y, Ouvrard G, Moreau P and Natoli C R 1997 *Phys. Rev.* B **55** 9508

[13] Sharma S, Nautiyal T, Singh G S and Auluck S 1999 *Phys. Rev.* B **59** 14833
[14] Reshak A H and Auluck S 2003 *Phys. Rev.* B **68** 245113
[15] Abbott E E, Kolis J W, Lowhorn N D, Sams W and Tritt T M 2004 *Mater. Res. Soc. Symp.* P **793** 295
[16] Kukkonen C A, Kaiser W J, Logothetis E M, Blumenstock B, Schroeder P A, Faile S P, Colella R and Gambold J 1981 *Phys. Rev.* B **24** 1691
[17] Whittingham M S 1978 *Prog. Solid State Chem.* **12** 41
[18] Mao Z and White R E 1993 *J. Power Sources* **43** 181
[19] Bruce P G and Saidi M Y 1992 *J. Electroanal. Chem.* **322** 93
[20] Thompson A H 1978 *Phys. Rev.* L **40** 1511
[21] Julien C M 2003 *Mater. Sci. Eng.* R **40** 47
[22] Suzuki K, Nakamura O, Kondo T and Enoki T 1996 *J. Phys. Chem. Solids* **57** 1133
[23] Imai H, Shimakaua Y and Kubo Y 2001 *Phys. Rev.* B **64** 241104
[24] Li D, Qin X Y, Zhang J, Wang L and Li H J 2005 *Solid State Commun.* **135** 237
[25] Li D, Qin X Y, Liu J and Yang H S 2004 *Phys. Lett.* A **328** 493
[26] Ong E W, McKelvy M J, Ouvrard G and Glaunsinger W S 1992 *Chem. Mater.* **4** 14
[27] Kobayashi H, Sakashita K, Sato M, Nozue T, Suzuki T and Kamimura T 1997 *Physica* B **169–171** 237
[28] Titov A N, Kuranov A V and Pleschev V G 2001 *Phys. Rev.* B **63** 035106
[29] Klipstein P C, Bagnall A G, Liang W Y, Marseglia E Z and Friend R H 1981 *J. Phys. C: Solid State Phys.* **14** 4067
[30] Klipsteint P C and Friend R H 1987 *J. Phys. C: Solid State Phys.* **20** 4169
[31] Julien C and Samaras I 1992 *Phys. Rev.* B **45** 13390
[32] Wu Z Y, Lemoigno F, Gressier P, Ouvrard G, Moreau P, Rouxel J and Natoli C R 1996 *Phys. Rev.* B **54** 11009